

Production of excited Rh atoms via keV particle bombardment of Rh{100}: Simulation of excitations due to collisions above the surface

Dan N. Bernardo and Barbara J. Garrison

Department of Chemistry, Pennsylvania State University, University Park, Pennsylvania 16802

(Received 20 July 1992; accepted 29 July 1992)

The production of atoms in the first excited state ($^4F_{7/2}$) of Rh via collisions 1.5–20 Å above the surface is studied. A method for efficiently simulating the contribution of excited atoms produced by this mechanism to the total yield of excited atoms is developed. Resulting velocity- and angle-resolved distributions are in good agreement with experimental results from previous studies.

I. INTRODUCTION

The excitation, deexcitation, and collisional processes that take place in a solid upon keV particle bombardment produce characteristic velocity and angular distributions of the atoms ejected in excited states.^{1–5} Comparison of these experimentally measured distributions with the results of theoretical predictions allows the development of increasingly detailed models of the processes which produce these excited atoms.⁶ One widely used model, proposed by Hagstrum,⁷ assumes that an atom can be excited at the surface and undergo deexcitation as it leaves the solid. The rate of deexcitation depends on the interaction between the excited atom and the substrate electrons and is assumed to vary exponentially with the height above the surface. The model predicts that the velocity dependence of the excitation probability P should behave as $\exp(-A/av_1)$, where v_1 is the component of escape velocity perpendicular to the surface and A/a is the deexcitation coefficient. This relation has been used to describe experimental distributions except for the low velocity regime where surface binding energy effects are suggested to alter this dependence.^{3,8}

Experimental determinations^{1,6} of the distributions of Rh atoms in the $^4F_{7/2}$ excited state indicate that the excitation probability is indeed exponentially dependent upon $(-1/v_1)$ at high ejection velocities. However, there are two differences between the experimental findings and the predictions of the Hagstrum model. First, the value of P approaches some constant value at low velocities. Second, the value of A/a has a dependence on the polar and azimuthal angles of ejection.

Explanations for these differences between experiment and the Hagstrum theory are obtained by combining molecular dynamics simulations of the keV particle bombardment process with a model for describing the excitation and subsequent deexcitation of atoms.^{1,6} The simulations are carried out as follows. A trajectory is initiated by aiming a high-velocity particle at a target consisting of ~ 1000 Rh atoms. The sequence of atomic collisions inside the solid is allowed to develop, with subsequent ejection of some of the Rh atoms. During the collision cascade, the excitation probability of an atom is set to some initial value P_0 if the distance between it and any of its neighbors is less than some threshold distance r_{th} . The excitation probability is assumed to decay via coupling with the electrons in

the solid as the atom continues its motion through the solid and possibly into the region above the surface. The lifetime for the decay process is considered to be constant in the solid and exponentially proportional to height in the region above the surface. The final ejection velocities and angles as well as excitation probabilities are recorded. Results from 4000 trajectories are combined to obtain statistically reliable velocity and angular distributions of atoms in the excited and ground states.

Results of the simulations indicate that atoms can undergo excitation in two distinct velocity regimes. At high ejection velocities, collisions with atoms at the surface produce most of the excited atoms. The deexcitation process starts when these atoms are close to the surface, and the final excitation probability becomes exponentially dependent on $-1/v_1$. At low ejection velocities, atoms excited at the surface experience considerable deexcitation during the ejection process, and their contribution to the total yield of excited atoms is small. Roughly half of the excited atoms are instead produced by collisions a few angstroms above the surface. Since the excitations for these atoms occur in a region where the electron density is approaching zero, there is practically no subsequent deexcitation. It is this latter mechanism which leads to an excitation probability which is independent of velocity. Thus, the simulations successfully predict the velocity dependence of the excitation probability over the whole range of experimentally observed velocities.

The simulations are less successful, however, in predicting the angular dependence of the excitation probability. The variation of P with angle was particularly difficult to predict at low velocities. In this regime, about half of the excited atoms are produced via collisional excitations a few angstroms above the surface. Several thousand of these atoms must be produced in the simulations in order to obtain statistically reliable angular distributions. Unfortunately, molecular dynamics calculations as outlined above are not particularly efficient in simulating collisions above the surface, since most of the computational effort is spent in simulating the collision cascade that occurs below the surface. For example, 4000 trajectories produce less than a hundred instances of collisional excitation above the surface. This small number means that insufficient collisions are present to allow prediction of the angular dependence of the excitation probability at low ejection velocities. A

more efficient method of simulating collisions above the surface is thus necessary to obtain results on the angular distributions of the excited atoms.

In this study, an efficient method for the simulation of atomic collisions a few angstroms above the surface is developed. This method is then used to simulate the collisional excitation of atoms, the results of which are used to obtain velocity- and angle-resolved distributions of Rh atoms in the first electronically excited state and in the ground state ($^4F_{7/2}$ and $^4F_{9/2}$, respectively). With this improved approach it is now possible to examine the angular dependence of the excitation probability over a wide range of ejection velocities. The importance of collisional excitations above the surface (relative to excitations at the surface) is also examined as a function of ejection velocity and angle.

II. THEORY

The simulation of atomic collisions a few angstroms above the surface consists of first selecting two atoms and assigning them initial ejection angles, velocities, and ejection times. The existence of a collision and the resulting final ejection angles and velocities can then be calculated. All these procedural steps are discussed in this section.

To select the atoms which eject from the surface, one can use a distribution $J(n)$, which gives the probability that the n th atom in the target will be ejected. Since this study deals with collisions of one atom with another, this distribution should not include the probability that an atom will be ejected as part of a cluster or the probability that only one atom will be ejected in a given trajectory. These constraints can be incorporated into the construction of $J(n)$ by using the distributions from previous molecular dynamics simulations.⁶ The resulting distribution is shown in Fig. 1. Once $J(n)$ is known, two atoms can then be picked independently.

The assignment of initial ejection velocities and angles to these chosen atoms is accomplished by using $S(v, \theta, \phi)$, the probability that an atom is ejected with velocity v , polar angle θ , and azimuthal angle ϕ . In the calculations, this distribution is expressed as

$$S(v, \theta, \phi) = S_v(v) S_a(\theta, \phi), \quad (1)$$

where $S_v(v)$, the velocity distribution, and $S_a(\theta, \phi)$, the angular distribution, are both obtained from previous experimental measurements.^{1,9} These distributions are shown in Figs. 2 and 3.

Since it is known that high-velocity atoms are generally ejected earlier in the cascade than low-velocity atoms,¹⁰ the time at which an atom leaves the surface must also be determined. This relation can be expressed in terms of the distribution $T(v, t)$, which gives the probability that an atom ejected with velocity v will leave the surface at time t . This distribution is obtained from previous molecular dynamics simulations⁶ and is shown in Fig. 4.

It is interesting to note that two of the above distributions are obtained from results of molecular dynamics simulations and not from experiments. The constraints re-

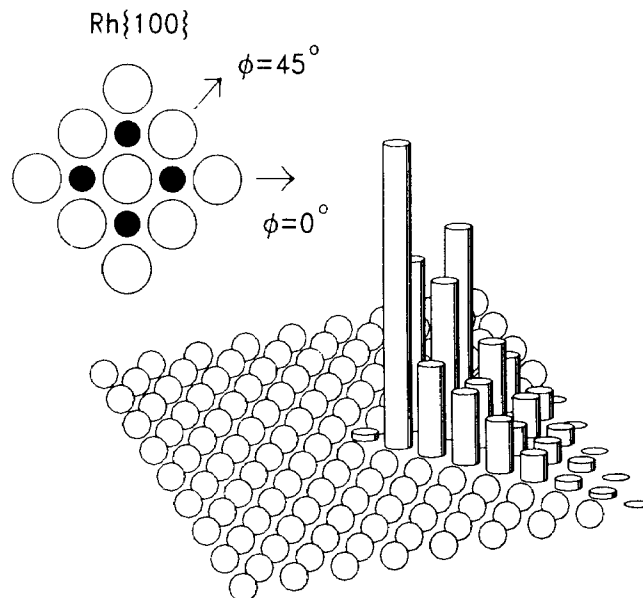


FIG. 1. First layer of the Rh{100} face. The bombarding particle strikes the atom in the center of the surface. A section of the surface is replaced by a histogram showing the ejection probability of an atom, $J(n)$. Since the surface has D_{4h} symmetry (see inset), values of $J(n)$ for one symmetry-unique section are shown. The azimuthal angles are defined in the inset. The value of $\phi = 0^\circ$ corresponds to the $\langle 100 \rangle$ direction while the $\phi = 45^\circ$ azimuth is also known as the $\langle 110 \rangle$ direction.

quired in the construction of $J(n)$ and the accuracy of the time correlation in $T(v, t)$ both preclude the determination of these distributions from current experimental measurements.¹¹ On the other hand, $S(v, \theta, \phi)$ is easily obtained by both theoretical and experimental means. The experimen-

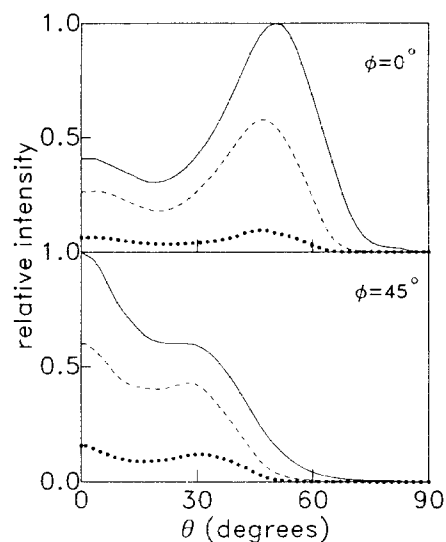


FIG. 2. Values of $S(v, \theta, \phi)$ as a function of the polar angle of ejection, θ . Distributions for $\phi = 0^\circ$ and $\phi = 45^\circ$ are shown. In this and all subsequent similar figures the solid line is used for representing the distribution of atoms with energies between 5 and 10 eV, the dashed line for energies of 10–20 eV, and the dotted line for energies of 20–50 eV.

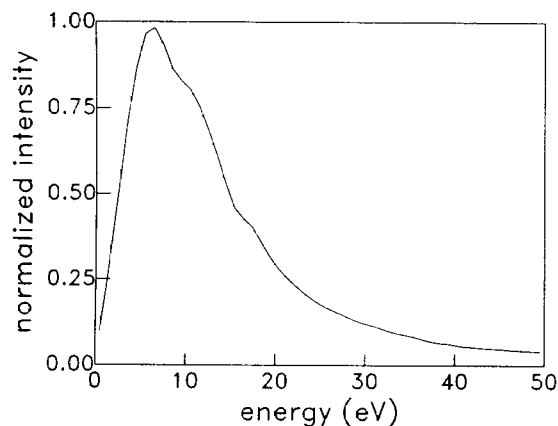


FIG. 3. Energy distribution of ejected atoms, obtained by integrating $S(v, \theta, \phi)$ over all ejection angles and converting velocities to energies.

tal distributions are statistically more reliable and are thus used.

A number of assumptions have been made in constructing and using the above distributions. For example, the ejection of each atom is assumed to be an event which is independent of the ejection of other atoms in the target. The distributions $J(n)$ and $T(v, t)$ were constructed from a sample set of a few thousand ejected atoms, and the detailed study of correlations with a small sample size was not attempted. Incorporation of all correlations is equivalent to repeating the original molecular dynamics simulations, which in turn would defeat the purpose of developing a computationally efficient method for studying collisions a few Angstroms above the surface.

Two other assumptions are used in the construction of $J(n)$. First, it is assumed that an atom is in its equilibrium position when it starts to leave the crystal. The displacement of atoms which are driven into the crystal and are later ejected at some other location on the surface are not

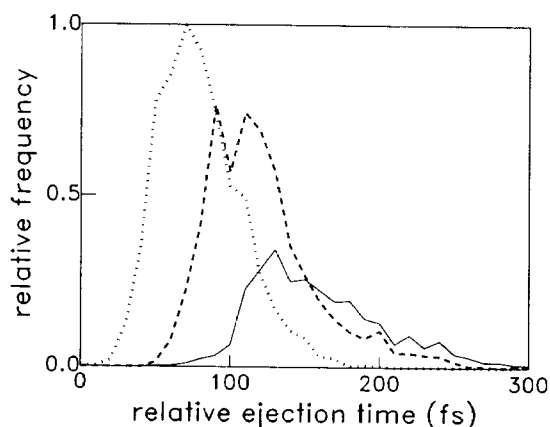


FIG. 4. Relative frequency of ejection, $T(v, t)$, as a function of ejection time t . The time $t=0$ is the point at which the primary particle first interacts with the solid. The solid line represents the distribution for atoms ejected with energies between 5 and 10 eV. The dashed line corresponds to atoms with energies of 10–20 eV; the dotted line, atoms with energies of 20–50 eV.

taken into consideration. Second, it is assumed that clusters are not involved in collisions above the surface.

Once the initial velocities, angles, and ejection times of the two atoms are determined, the Rh dimer potential¹² from the same potential as used in the molecular dynamics simulation⁶ is used to determine the distance of closest approach, r_c . If r_c is less than the threshold distance for excitation, r_{th} , then the velocities and angles of the two atoms after the collision as well as the height z_i at which the collision occurs are calculated.^{13,14} If the height is above some minimum value z_{i0} , then both initial and final sets of velocities and angles are recorded.

The above procedure is iterated, each time for a new pair of ejecting atoms, until a sufficient number of collisions has occurred to allow the determination of $C(v, \theta, \phi)$, the velocity and angular distribution of atoms that have experienced a collision above the surface. The population of excited state atoms produced by collisions above the surface is given by

$$N_c^*(v, \theta, \phi) = C(v, \theta, \phi) P_0, \quad (2)$$

where P_0 is the initial value of the excitation probability as determined in Ref. 6. The corresponding population of atoms in the ground state is obtained using

$$N_c(v, \theta, \phi) = C(v, \theta, \phi) (1 - P_0). \quad (3)$$

In order to obtain the total populations of atoms in the excited and ground states, one must also include the contribution of atoms which are ejected and do not experience any collisions above the surface. The population of excited state atoms produced by collisions at the surface is given by

$$N_s^*(v, \theta, \phi) = S(v, \theta, \phi) P(v, \theta, \phi), \quad (4)$$

where $P(v, \theta, \phi)$ is the excitation probability for an atom ejected at the surface with velocity v , polar angle θ , and azimuthal angle ϕ . [The determination of $P(v, \theta, \phi)$ will be discussed later in the section.] The corresponding population of ground state atoms is

$$N_s(v, \theta, \phi) = S(v, \theta, \phi) [1 - P(v, \theta, \phi)]. \quad (5)$$

The total populations of atoms in the excited and ground states are finally obtained by

$$N^*(v, \theta, \phi) = N_c^*(v, \theta, \phi) + N_s^*(v, \theta, \phi) \quad (6)$$

and

$$N(v, \theta, \phi) = N_c(v, \theta, \phi) + N_s(v, \theta, \phi). \quad (7)$$

The populations of atoms in the excited and ground states can be predicted if $P(v, \theta, \phi)$ is known. In this study it shall be assumed that the azimuthal dependence can be neglected, i.e., $P(v, \theta, \phi) \approx P(v, \theta)$. In a previous study⁶ we have found that the values of $P(v, \theta)$ are related to v_{max} , the maximum value of the normal component of the velocity that an atom attains as it leaves the surface, via

$$P(v, \theta) = g \exp(-h/v_{max}), \quad (8)$$

where g and h are fitting parameters. The value of v_{max} is in general larger than the measured quantity of v_1 because the atom must overcome the surface binding energy in order to

eject. If one assumes ejection from a quiescent surface so that the surface binding energy E_b is uniquely defined, the value of v_{\max} can be easily calculated using

$$v_{\max} = (v_1^2 + 2E_b/m)^{1/2}, \quad (9)$$

$$v_1 = (2E/m)^{1/2} \cos \theta, \quad (10)$$

where m is the atomic mass and $E_b = 5.75$ eV (corresponding to a velocity of 0.33×10^6 cm/s) for Rh.¹⁵ Using this method of calculating v_{\max} , the values of g and h are adjusted so that the theoretically predicted magnitude N^*/N and slope $d(\log(N^*/N))/d(1/v_1)$ match the experimental values in the high-velocity limit for atoms ejected in the normal ($\theta < 10^\circ$) direction. This fitting procedure yields values of $g = 1.3$ and $h = 1.9 \times 10^6$ cm/s. It must be emphasized that these two parameters are in no way related to the calculation of excitations via collisions a few angstroms above the surface, and that this is the only curve fitting done in this study.

III. RESULTS AND DISCUSSION

In this section the velocity and angular distributions of Rh atoms in the $^4F_{9/2}$ and $^4F_{7/2}$ states as obtained from these model simulations will be examined. These results should give new insight into features such as the experimentally determined nonexponential behavior of N^*/N at low velocities. The simulations also allow examination of various excitation events on the atomic scale. For example, the origins of the excited atoms can be examined. In the framework of the current model, some of the excited atoms will be produced by collisions at the surface while others will undergo collisional excitation above the surface. It is thus necessary to first determine the range of heights which define "collisions above the surface."

A. Range of heights studied

Over what range of heights (z_{lo} , z_{hi}) should collisions be studied? The value of the lower limit, z_{lo} , is of considerable importance. It must be sufficiently low so as not to omit the majority of collisions occurring near the surface. The frequency of collisions as a function of z is shown in Fig. 5. It can be seen that most of the collisions occur at small values of z . The integral of the frequency is also plotted, and this shows that 50% of all collisions above the surface occur for $z < 4$ Å. Thus, the value of z_{lo} must be well below 4 Å.

On the other hand, the value of z_{lo} must also be sufficiently high so that the colliding atoms should no longer experience the surface binding energy. Figure 3 in Ref. 6 shows that the atom is free of this binding energy and attains its final velocity at ~ 1.5 Å above the surface. We therefore assign $z_{lo} = 1.5$ Å, and use this value in all subsequent calculations and discussions.¹⁶

The value of the upper limit, z_{hi} , is not as important as that of z_{lo} since one would expect the frequency of collisions to rapidly decrease with increasing z . This trend is indeed seen in Fig. 5, and so all results were calculated with $z_{hi} \rightarrow \infty$. However, a finite value for the upper limit is repeatedly mentioned in the discussion in order to empha-

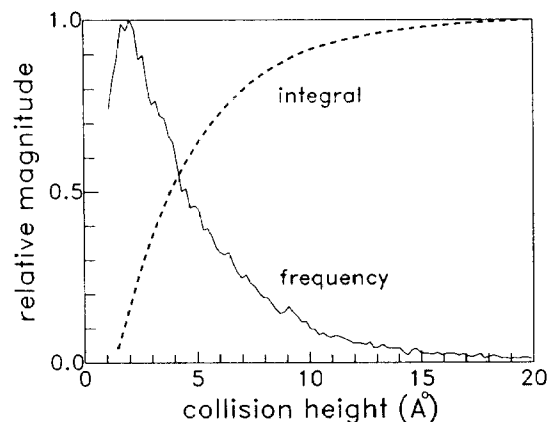


FIG. 5. Frequency of collisions as a function of collision height. The integral of the frequency (integration was started at $z = 1.5$ Å) is shown as the dashed line.

size the fact that most of the collisions occur close to the surface. Additional calculations indicate that 98% of all atoms colliding with $z_i \geq 1.5$ Å also satisfy the condition $z_i \leq 20$ Å, and thus we refer to collisions above the surface as those occurring "1.5–20 Å above the surface."

B. Velocity and angular distributions

The angular distribution of excited atoms ejected along the $\phi = 0^\circ$ azimuth is shown in Fig. 6. The analogous distribution for atoms ejected along the $\phi = 45^\circ$ azimuth is shown in Fig. 7. Both sets of experimental and theoretical distributions indicate a greater tendency for ejection in the normal direction when compared to the distributions of ground state atoms. An explanation for this difference can be obtained if the total excited state distribution N^* from

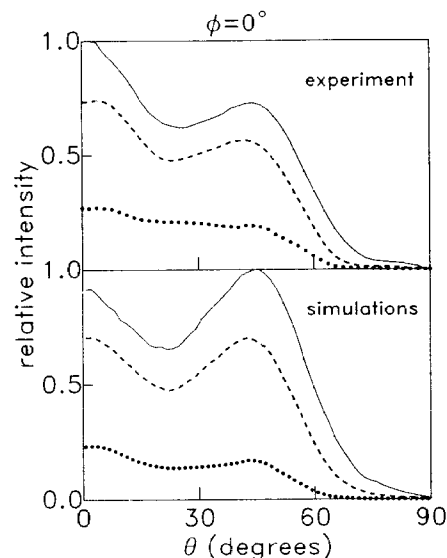


FIG. 6. Angular distribution of excited atoms ejected along the $\phi = 0^\circ$ azimuth. Results of experiments and simulations are shown for the same ranges of energy as in Fig. 2.

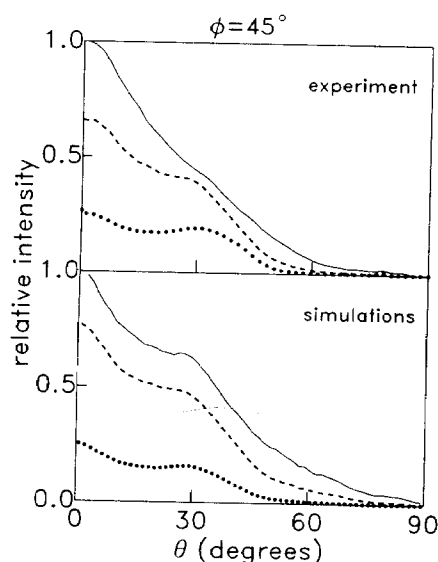


FIG. 7. Angular distribution of excited atoms ejected along the $\phi=45^\circ$ azimuth. Results of experiments and simulations are shown for the same ranges of energy as in Fig. 2.

the simulations is broken down into N_c^* , the contribution from atoms excited 1.5–20 Å above the surface, and N_s^* , the contribution from excitations at the surface. Examples of this decomposition are shown in Fig. 8. The distributions for N_c^* are relatively featureless while those for N_s^* exhibit a dependence on polar angle. Thus, angular variations in N^* can be attributed to N_s^* . The expression for N_s^* [Eq. (4)] shows that this is proportional to $P(v, \theta, \phi)$, which in turn behaves as $\sim \exp(-1/v \cos \theta)$. An atom ejecting in the normal direction will have higher values of v_\perp [and consequently $P(E, \theta)$] than an atom with the same

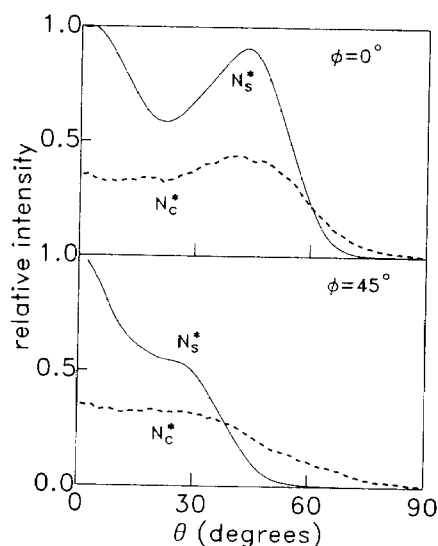


FIG. 8. Separation of angular distribution of excited atoms into contributions from collisions at the surface (solid line) and collisions above the surface (dotted line). Results for atoms ejected along the two azimuthal directions ($\phi=0^\circ$ and $\phi=45^\circ$) with energies from 10–20 eV are shown.

energy which is ejected in the off-normal direction. This causes the angular distributions for atoms in the excited state to exhibit a propensity for ejection in the direction normal to the surface.

C. Variation of the excitation probability with ejection velocity and angle

The exponential-like behavior of the excitation probability can be seen by examining the logarithm of the ratio of the measured intensities, $\log(N^*/N)$, as a function of $1/v_\perp$. Plots comparing the theoretical and experimental results are presented in Figs. 9(a) and 9(b). Data for six polar angle intervals and two azimuthal directions are shown.

There is good agreement between the theoretical and experimental results. Both sets of results exhibit values of N^*/N that vary as $\exp(-A/av_\perp)$ at high velocities and then reach some constant value at low velocities. The agreement between experiment and theory for data on high-velocity atoms ejected normal to the surface ($\theta < 10^\circ$) is due to the fitting procedure mentioned in Sec. II. The experimental data at this point was used to determine the values of the constants g and h in Eq. (8). However, these constants are not used in calculating excitation probabilities of atoms which undergo collisional excitation 1.5–20 Å above the surface. Thus, the fitting procedure does not influence the velocity dependence of the excitation probability at lower velocities. The particularly good agreement between theory and experiment for the particles ejected with $\theta > 20^\circ$ is an indication of the validity of the model in predicting the yield of excited atoms over a wide range of ejection angles and velocities.

Another test of the model involves its prediction of the low-velocity value of N^*/N as a function of ejection angle. The theoretical results show that, at low velocities, N^*/N stays at some constant value. This value decreases with increasing θ for the $\phi=0^\circ$ azimuth but remains constant for the $\phi=45^\circ$ azimuth. These results are in agreement with the experimental results, and can be explained by examining the angular distributions of the low-velocity atoms ejected in the excited and ground states. We first consider the polar angle distribution of atoms in the excited state. The distribution of atoms in the excited state decreases with increasing θ for both $\phi=0^\circ$ and $\phi=45^\circ$ azimuths (Figs. 6 and 7). Likewise, ground-state atoms which are ejected along the $\phi=45^\circ$ azimuth (Fig. 2) have a distribution which decreases with increasing θ , and so the ratio N^*/N remains constant over all θ for $\phi=45^\circ$. However, the distribution of ground-state atoms along the $\phi=0^\circ$ azimuth (Fig. 2) exhibits a markedly different dependence on the polar angle of ejection. This distribution has a maximum at $\theta \approx 50^\circ$, which has been attributed to the focused ejection of a first layer atom.⁹ This causes the polar angle distribution to increase with θ until $\theta \approx 50^\circ$, which in turn causes the ratio N^*/N to decrease with θ for this azimuth. Thus the results of the simulations account for the experimentally observed trends over most of the ejection angles.

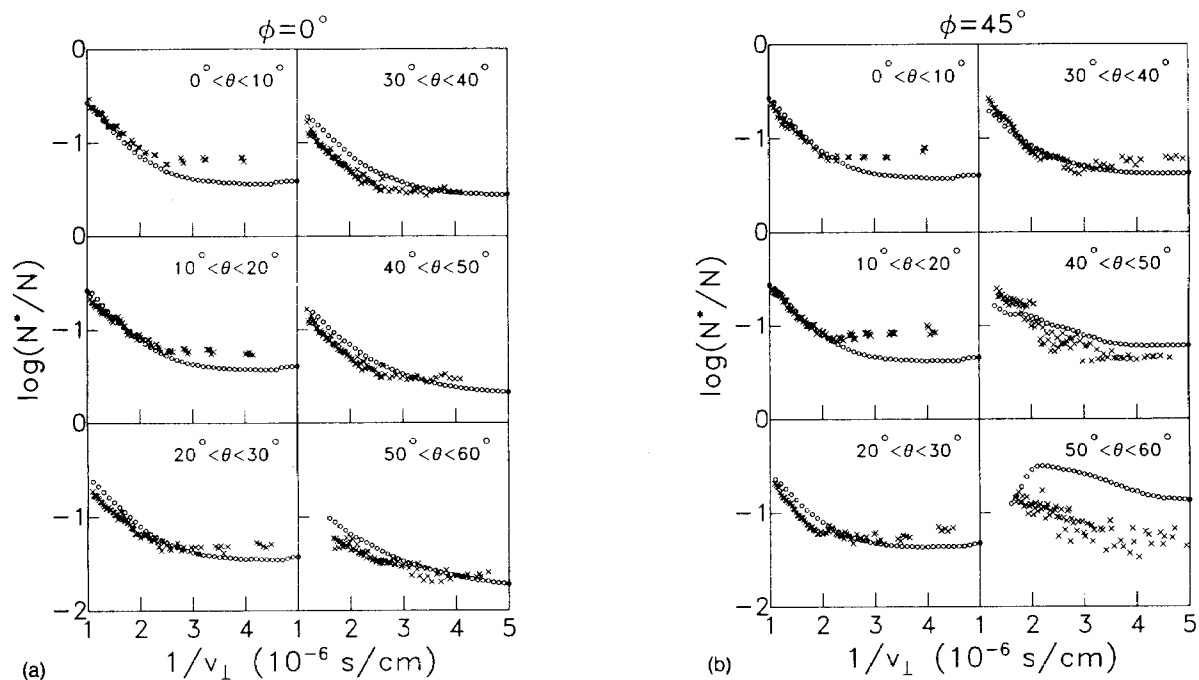


FIG. 9. Logarithm of the ratio of the measured intensities, $\log(N^*/N)$, vs $1/v_{\perp}$ for different angles of ejection. Data for six polar angle intervals are shown. Crosses represent experimental results, and circles represent theoretical predictions. (a) Results for atoms ejected along the $\phi=0^{\circ}$ azimuth. (b) Results for atoms ejected along the $\phi=45^{\circ}$ azimuth. A value of $1/v_{\perp}=2 \times 10^{-6}$ s/cm for ejection normal to the surface corresponds to an energy of 13 eV.

The agreement between our model calculations and the experimental values is not perfect. One problem exists for low-velocity atoms ejected with $50^{\circ} < \theta < 60^{\circ}$ along the $\phi=45^{\circ}$ azimuth. This difference is probably due to the large uncertainty in N^*/N caused by taking the quotient of two distributions, both of which are approaching zero at large polar angles along this azimuth. Two other differences between the theoretical and experimental values of N^*/N are (a) the simulations underestimate the low-velocity values for $\theta < 20^{\circ}$, and (b) the simulations predict a slightly more gradual transition in the velocity dependence (from being exponential-like to being independent of the velocity). Explanations for these differences have not been obtained in additional calculations using the current model. Perhaps more detailed treatments of the excitation and deexcitation mechanisms, such as incorporation of azimuthal dependence into the expression for $P(v, \theta)$ [Eq. (8)] will provide answers. In spite of these differences, the agreement between theory and experiment over a wide range of ejection velocities and angles suggests that the simple model used in this study adequately describes the general excitation and deexcitation mechanisms that take place during the ejection of target atoms.

In addition to examining the velocity and angular dependence of N^*/N , the simulations allow us to examine the relative contributions of N_c^*/N and N_s^*/N to the ratio N^*/N . These contributions can be seen as a function of velocity in Fig. 10. Results for three different angles of ejection are shown. Examination of these results yields a few interesting observations. First, the value of N_c^*/N remains constant over the whole range of ejection velocities and angles.

Second, the relative magnitudes of N_c^* and N_s^* vary with ejection angle, with the former becoming more important at velocities below 2.6×10^6 – 3.6×10^6 cm/s. It is this larger contribution of N_c^* to N^* at low velocities which leads to

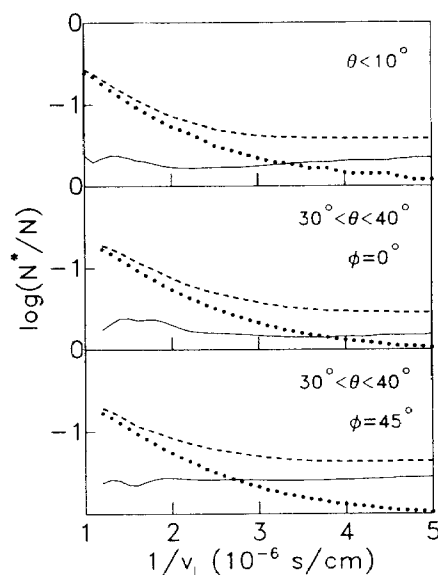


FIG. 10. Separation of N^*/N into its contributions from atoms excited at various heights. Theoretical predictions are for atoms ejected with energies from 10–20 eV. Results for ejection along three different directions are shown. The dashed line represents $\log(N^*/N)$, where N^* is the total population of excited atoms. The solid line corresponds to $\log(N_c^*/N)$, where N_c^* is the population of excited atoms produced by collisions 1.5–20 Å above the surface. The dotted line represents $\log(N_s^*/N)$, where N_s^* is the population of excited atoms produced by collisions at the surface.

the leveling off of N^*/N at some constant value. Third, at low velocities the ratio N_s^*/N exhibits some curvature (due to the surface binding energy) but does not level off. This means that if collisions at the surface were the only source of atomic excitations, the resulting N^*/N (which would then be equal to N_s^*/N) would not become constant at low velocities. This analysis clearly illustrates the importance of excited atoms produced by collisional excitation 1.5–20 Å above the surface.

In summary, the combination of a collisional excitation mechanism with simulations of collisions 1.5–20 Å above the surface yields velocity- and angle-resolved distributions which are in good agreement with experimental findings. The results account for the variation of the excitation probability over a wide range of ejection velocities and angles, and illustrate the importance of collisions above the surface as a process for producing the majority of excited atoms at low velocities. The abundance of information and insight obtained in this study is remarkable considering the simplicity of the model and the use of only two fitting parameters, both of which are unrelated to the calculation of excitations via collisions above the surface.

ACKNOWLEDGMENTS

We gratefully acknowledge the financial support of the National Science Foundation and the Office of Naval Research. The Pennsylvania State University supplied a generous grant of computer time for this study.

- ¹ N. Winograd, M. El-Maazawi, R. Maboudian, Z. Postawa, D. N. Bernardo, and B. J. Garrison, *J. Chem. Phys.* **96**, 6314 (1992).
- ² G. Betz, *Nucl. Instrum. Methods B27*, 104 (1987), and references therein.
- ³ M. L. Yu and N. D. Lang, *Phys. Rev. Lett.* **50**, 127 (1983).
- ⁴ G. E. Young, M. F. Calaway, M. J. Pellin, and D. M. Gruen, *J. Vac. Sci. Technol. A* **2**, 693 (1984).
- ⁵ W. Heiland, J. Kraus, S. Leung, and N. H. Tolk, *Surf. Sci.* **67**, 437 (1977).
- ⁶ D. N. Bernardo, M. El-Maazawi, R. Maboudian, Z. Postawa, N. Winograd, and B. J. Garrison, *J. Chem. Phys.* **97**, 3846 (1992).
- ⁷ H. D. Hagstrum, *Phys. Rev.* **96**, 336 (1954).
- ⁸ J. H. Lin and B. J. Garrison, *J. Vac. Sci. Technol. A* **1**, 1205 (1983).
- ⁹ R. Maboudian, Z. Postawa, M. El-Maazawi, B. J. Garrison, and N. Winograd, *Phys. Rev. B* **42**, 7311 (1990).
- ¹⁰ R. P. Webb and D. E. Harrison, *Vacuum* **34**, 847 (1984).
- ¹¹ One might speculate on the possibility of performing coincidence experiments to obtain these distributions. See, for example, M. A. Park, K. A. Gibson, L. Quinones, and E. A. Schweikert, *Science* **25**, 988 (1990), and references therein.
- ¹² B. J. Garrison, N. Winograd, D. M. Deaven, C. T. Reimann, D. Y. Lo, T. A. Tombrello, D. E. Harrison, Jr., and M. H. Shapiro, *Phys. Rev. B* **37**, 7197 (1988).
- ¹³ F. J. Smith, *Physica* **30**, 497 (1964).
- ¹⁴ H. O'Hara and F. J. Smith, *J. Comput. Phys.* **5**, 328 (1970).
- ¹⁵ C. Kittel, *Introduction to Solid State Physics*, 6th ed. (Wiley, New York, 1986), p. 55.
- ¹⁶ The use of $z_{10} = 1.5$ Å implies that the ejecting atoms which undergo excitation close to the surface will experience some degree of deexcitation afterwards, leading to a final excitation probability that is less than P_0 [i.e., Eq. (2) no longer holds]. Additional calculations show that the deexcitation in this case causes the average excitation probability to decrease by less than 5%. Equation (2) becomes a good approximation and is still used in all calculations.